Performances of neutron cold multi-chopper instruments with different source natures among reactor, short and long pulse sources

Masatoshi Arai*

European Spallation Source ERIC, P.O. Box 176, 221 00 Lund, Sweden

Abstract. Cold multi-chopper instrument is a popular instrument commonly used for variety of scientific fields, built in reactors and sharp pulse sources and will be built in a long pulse source. In this article I compare the performance of those instruments, IN5 at ILL, AMATERAS at J-PARC and CSPEC at ESS, and show a merit/demerit come from the different characters of the source itself, and finally give a suggestion for a further improvement.

1 Introduction

Cold multi-chopper instrument is very popular and very useful, which serves a very important platform to study dynamical aspect of condensed matter in various scientific fileds. Its optimization scheme at reactor source was established in early 1990's [1], and since then relevant instruments have been constructed and operated at various kind of neutron sources. The design of the instrument is performed at a balance between two aspects, namely those are flux and resolution as a regular guideline. However, different characters of the source itself gives another dimension to be considered. Recent analysis on an expected performance of ESS instruments to ones at other sources with a different character stimulated us to revisit a way of optimization and use cases [2]. In this report, I present the consideration to optimize the performance of the relevant instruments at reactor (IN5), short-pulse (AMATERAS) and long-pulse (CSPEC), and show not only merit/demerit of source but also tunability emerged from the different source nature.

Here, we mostly focus on an argument for a typical use case (hereafter referred as "Typical Case") for E_i = *3 meV* (5Å) with resolution $\Delta\varepsilon / E_i = 3\%$ and angular divergence of $\Delta\theta = \pm 1.0°$, but extend to tunability by varying the energy resolution in the end.

2 Flux calculation

Figure 1 shows the time averaged brightness, B_{TA} [n/cm²/s/str/eV], of ESS (5MW), ILL (57MW) and J-PARC's coupled moderator (1MW) [2]. This is the important base information to go further, from which we can calculate flux at sample, once we know parameters of instrument such as energy range, energy resolution, angular divergence at sample. However, here we assume the brilliance transformation efficiency of guide system is perfect, $T_g = 1.0$, and we assume that there is no beam loss in it. Since it highly depends on the guide design, therefore, we neglect it for the time being, but it will be discussed in the later section.

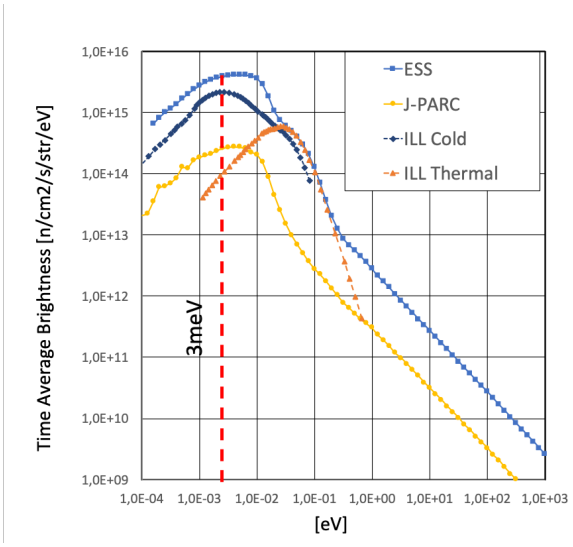

Fig. 1. Time averaged brightness of ESS (5 MW), ILL (57 MW) and J-PARC's coupled moderator (1 MW) [2]. In the report we will discuss for Ei = 3meV as Typical Case.

Fig. 2 shows a layout of a multi-chopper instrument. There are several time widths to be considered depending on sources. Those are,

- Δt_{MC}: chopper opening time of the monochromatic chopper (MC)
- Δt_{PSC}: chopper opening time of the pulse shaping chopper (PSC)
- Δt_m: pulse width at moderator

* Corresponding author: masatoshi.arai@ess.eu

Here, we assume an instrument at short pulse does not use PSC, although there is its option on AMATERAS. Also, all of widths are defined as a full width at half maximum of a peak structure.

There are also three key distances, d_1, d_2, and d_3. Those are:

- d_1: the primary distance from the source to MC for short pulse, and from PSC to MC for long pulse or reactor instrument.
- d_2: the secondary distance from sample to detector.
- d_3: the distance between MC and sample. Normally a shorter d_3 is better in terms of the resolution.

In case for a pulsed neutron source, nevertheless short or long pulse source, the flux at sample is approximately defined as,

$$F(E_i) = B_{TA}(E_i) \cdot (\Delta t_{ch}/\Delta t_m) \cdot \Delta E_i \cdot (2\Delta\theta_s)^2 \cdot T_B \quad (1)$$

where the monochromatic chopper cuts out the time width Δt_{ch} from the original width of Δt_m at moderator for a given energy E_i, giving the term $\Delta t_{ch}/\Delta t_m$ with the condition of $\Delta t_{ch} < \Delta t_{PSC} < \Delta t_m$. Practically it is $\Delta t_{ch} \ll \Delta t_m$ for long pulse and reactor sources. The angular divergence, $2\Delta\theta_s$, at sample should be less than that of the guide system and incident energy resolution ΔE_i is also much less than the available energy range of $B_{TA}(E_i)$.

On the other hand, in case for reactor source, PSC creates pulses at frequency of f, then the resultant pulse width can be defined as $\Delta t_m = 1/f$. Therefore, the flux is described as,

$$F(E_i) = B_{TA}(E_i) \cdot (\Delta t_{ch} \cdot f) \cdot \Delta E_i \cdot (2\Delta\theta_s)^2 \cdot T_B \quad (2)$$

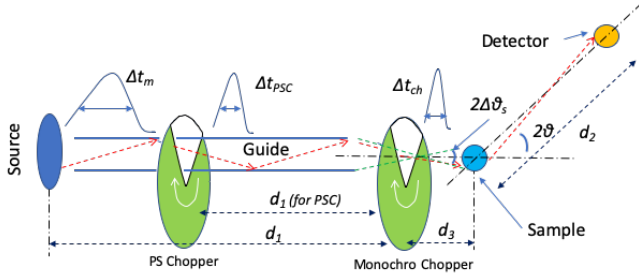

Fig. 2. Layout of a multi-chopper instrument. In case for a long pulse or a reactor source, a pulse shaping chopper (PSC) sharpens the pulse. And monochromatic chopper defines Ei in any sources.

The incident energy resolution ΔE_i after MC contains two components. One comes from MC's time width, Δt_{ch}, and another from that at the source or PSC, $\Delta t_{m/PSC}$.

$$\left(\frac{\Delta E_i}{E_i}\right)^2 = \left(2\frac{h}{m \cdot \lambda \cdot d_1}\right)^2 \left(\Delta t_{ch}{}^2 + \Delta t_{\frac{m}{PSC}}{}^2\right)$$
$$= \left(2\frac{0.3956}{\lambda \cdot d_1}\right)^2 \left(\Delta t_{ch}{}^2 + \Delta t_{m/PSC}{}^2\right) \quad (3)$$

Here, we define $\Delta t_{m/PSC}$ so as Δt_m is for short pulse source and Δt_{PSC} for long and continuous sources. The conversion factor 0.3956 is applied for distance in 'cm', time in 'μs' and wavelength λ in '$\AA$'.

The time of flight of neutrons is described as,

$$t[\mu s] = \frac{L}{v} = \frac{m \cdot \lambda \cdot L}{h} = \frac{\lambda[\text{Å}] \cdot L[cm]}{0.3956} \quad (4)$$

Therefore, from Eq. (3),

$$\Delta E_i = \frac{2\times 0.3956}{\lambda \cdot d_1} E_i \cdot \sqrt{\left(\Delta t_{ch}{}^2 + \Delta t_{m/PSC}{}^2\right)} \quad (5)$$

For a convention, we rewrite Eq. (5) as

$$\Delta E_i = D \cdot \sqrt{x^2 + y^2} \quad (6)$$

$$D = \frac{2\times 0.3956}{\lambda \cdot d_1} E_i, \ \Delta t_{ch} = x, \ \Delta t_{m/PSC} = y \quad (7)$$

3 Operation mode of instruments

Figure 3 shows a TOF-distance diagram of operation of multi-chopper instruments at different kind of sources (time of flight: TOF). At reactor, a set of PSC and MC extracts multi pulsed beams at the same incident energy with a frequency of f, called repetition rate multiplicity (RRM) [3]. At long pulse source, the chopper system is the same or similar as at reactor, but it extracts slightly different incident energies by RRM at a long flight distance from moderator to detector. The energy variation depends on the flight distance. At short pulse, only MC is needed to extract different incident energies, and creates well separated incident energies in most cases with a shorter d_3.

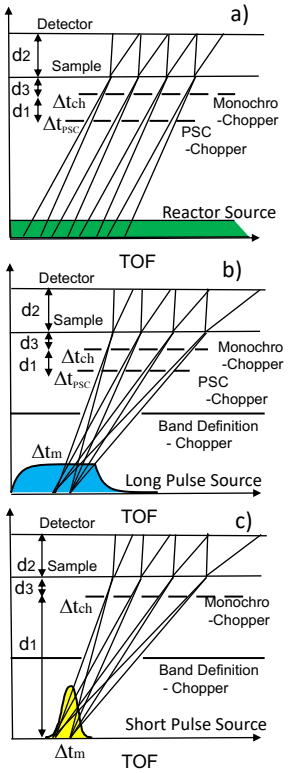

Fig. 3. Operation mode of multi-chopper instruments at different kind of sources. Reactor; a set of PSC and MC create monochromatic multi pulsed beam at a frequency of f. Long pulse source; it extracts RRM pulses with slightly different incident energies with a long flight distance. Short pulse; Only MC extracts well separated different incident energies.

This ability is preferably called "multi-Ei" a synonym of RRM developed on a Fermi-chopper instrument [4]. In the comparison in the next section, we mainly compare the RRM of IN5 at 142 Hz and single-mode (one of single incidence within RRM) of CSPEC and AMATERAS, where the source is operated at repetition rate of 14 Hz and 25 Hz respectively.

4 Resolution of a chopper instrument

The energy resolution of chopper instrument is described as Eq. (8) [5],

$$\frac{\Delta\varepsilon}{E_i} = \sqrt{\left\{\left[\frac{2\Delta t_{ch}}{t_{ch}}\left(1+\frac{d_1+d_3}{d_2}\left(1-\frac{\varepsilon}{E_i}\right)^{\frac{3}{2}}\right)\right]^2+\left[\frac{2\Delta t_{m/PSC}}{t_{ch}}\left(1+\frac{d_3}{d_2}\left(1-\frac{\varepsilon}{E_i}\right)^{\frac{3}{2}}\right)\right]^2\right\}} \quad (8)$$

However, in order to simplify the argument, here, we concentrate on the energy resolution at the elastic position ($\varepsilon = 0$), where most neutron intensity is counted, and we can analyze the major aspect of optimization. Therefore, the resolution formula at the elastic position can be written as follows,

$$R = \frac{\Delta\varepsilon}{E_i} = \frac{2\times0.3956}{d_1\cdot\lambda}\times \sqrt{\left\{\left[\Delta t_{ch}\left(\frac{d_1+d_2+d_3}{d_2}\right)\right]^2+\left[\Delta t_{m/PSC}\left(\frac{d_2+d_3}{d_2}\right)\right]^2\right\}} \quad (9)$$

The Parameters in Eq. (9) are depicted in Fig. 2. Eq. (9) is simplified as,

$$c^2 = \{(ax)^2+(by)^2\} \quad (10)$$

where,

$$x = \Delta t_{ch}, y = \Delta t_{m/PSC}$$

and

$$c = \frac{R\cdot d_1\cdot\lambda}{2\times0.3956}, a = \frac{d_1+d_2+d_3}{d_2}, b = \frac{d_2+d_3}{d_2} \quad (11)$$

This is converted and is a formula of an ellipse,

$$g = \left(\frac{a}{c}\right)^2 x^2+\left(\frac{b}{c}\right)^2 y^2 - 1 = Ax^2+By^2-1 = 0 \quad (12)$$

where,

$$A = \left(\frac{a}{c}\right)^2 = \frac{\left(\frac{d_1+d_2+d_3}{d_2}\right)^2}{\left(\frac{R\cdot d_1\cdot\lambda}{2\times0.3956}\right)^2}, B = \left(\frac{b}{c}\right)^2 = \frac{\left(\frac{d_2+d_3}{d_2}\right)^2}{\left(\frac{R\cdot d_1\cdot\lambda}{2\times0.3956}\right)^2} \quad (13)$$

5 Optimization Concepts

Here, we assume the geometrical parameters, such as d_1, d_2, and d_3 have been given for the time being, and optimization is a subject to determine the timing aspects. In case for a short pulse source Δt_m is given from the moderator characteristics for each energy, and cannot control from the instrument [2]. Therefore, Δt_{ch} is uniquely determined for the required energy resolution in Eq. (9). On the other hand, in a long pulse source or a reactor source, two chopper windows, Δt_{ch} and Δt_{PSC}, are tunable, and the optimization of the chopper opening time should be done by finding the maximum flux at sample by keeping a required resolution R through the constraint of Eq. (12).

5.1 Lechner's Optimization Concept

Lechner assumed the flux at sample is proportional to $\propto \Delta t_{ch}\cdot\Delta t_{PSC} = x\cdot y$ [1], [6]. This corresponds to the maximization of the area of,

$$S = x\cdot y \; for \; x,y \geq 0 \quad (14)$$

under the condition of Eq. (12) as shown in Fig. 4. The solution is given by the Lagrange multiplier method,

$$L(x,y) = S-\lambda\cdot g = x\cdot y-\lambda\cdot(Ax^2+By^2-1) \quad (15)$$

by taking partial derivatives to find local minima, $\frac{\partial L}{\partial x} = 0$, $\frac{\partial L}{\partial y} = 0$, and we can have the following solution.

$$x = \frac{1}{\sqrt{2A}}, \quad y = \frac{1}{\sqrt{2B}} \quad (16)$$

And the optimum opening time has a relation as,

$$\frac{x}{y} = \frac{\Delta t_{ch}}{\Delta t_{\mathrm{PSC}}} = \sqrt{\frac{B}{A}} = \frac{d_2+d_3}{d_1+d_2+d_3} \quad (17)$$

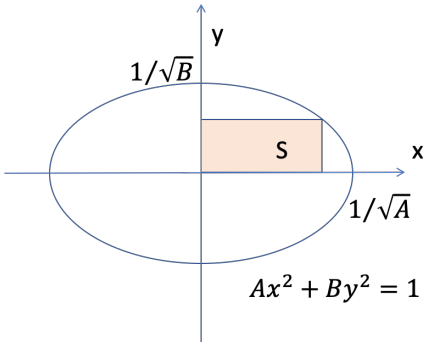

Fig. 4. Ellipse of Eq. (12). Maximizing "S" of Eq. (14) is subject.

5.2 Another Optimization concept

As we expressed in Eq. (1), Eq. (2) and Eq. (6) under a given beam divergence, $2\Delta\theta_s$ the flux at sample is proportional to,

$$flux \propto \frac{\Delta t_{ch}}{\Delta t_m}\cdot\Delta E_i = \frac{\Delta t_{ch}}{\Delta t_m}\cdot D\cdot\sqrt{\Delta t_{\mathrm{ch}}{}^2+\Delta t_{\mathrm{PSC}}{}^2} \propto f = x\sqrt{x^2+y^2} \quad (18)$$

where we left only relevant terms, x and y, in the rightmost equation, since Δt_m and D is given from the source character, and d_i and E_i are also given. Now we maximize Eq. (18) under a constraint of Eq. (12) by Lagrange's multiplier method;

$$L(x,y) = f-\lambda\cdot g = x\sqrt{x^2+y^2}-\lambda(Ax^2+By^2-1) \quad (19)$$

The solution is following,

$$x = \sqrt{1/2(A-B)},\ y = \sqrt{(A-2B)/(2B(A-B))} \quad (20)$$

namely,

$$x/y = \sqrt{B/(A-2B)} \quad (21)$$

This contrasts with Lechner's result, $x/y = \sqrt{B/A}$, Eq.(17). A correction term "2B" comes into the denominator in Eq. (21).

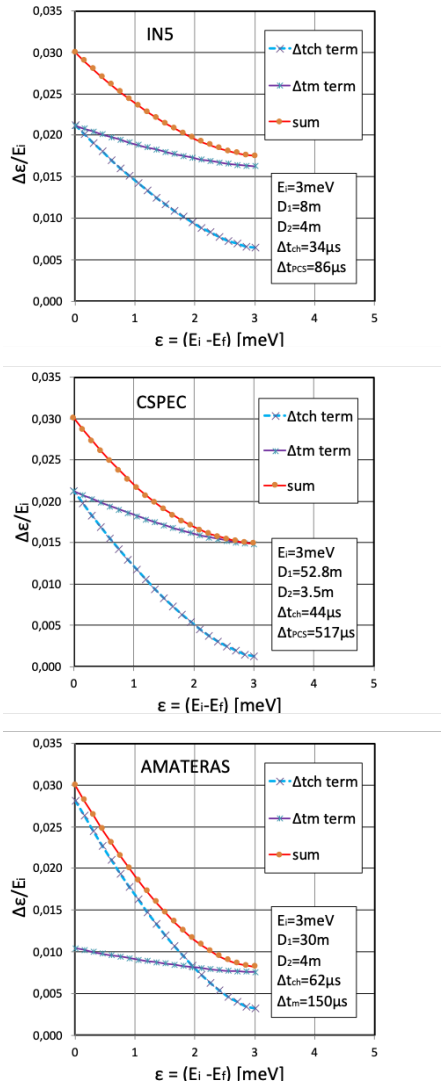

Fig. 5. Lechner's optimization; Energy resolution diagram for CSPEC, AMATERAS and IN5, where Δε/Ei is kept at 3% at the elastic position. In each panel, the first term with (Δtch), the second term with (Δtm/PSC) in Eq. (8) and the sum of them are depicted.

Lechner's results gives that a matching condition for the partial resolution regarding Δt_{ch} and Δt_{psc} and the first and the second term of Eq. (9) have the same value at the elastic position as shown in Fig. 5 for CSPEC and IN5. Fig. 5 was calculated by Eq. (8) in the applicable energy transfer range up to $\varepsilon = E_i$.

On the other hand, the resolution diagram for the present optimization is shown in Fig.6. CSPEC does not have significant change in the diagram because d_i is relatively very longer than d_2 and d_3. However, the diagram of IN5 shows a minor but definite difference by the correction term in Eq. (21) as shown at the elastic position in Fig.6.

AMATERAS has decisive value, x = Δt_{ch}, determined by a required resolution with a given y = Δt_m as shown in Eq. (22), and there is no difference whatever the optimization method, and the resolution diagram is only shown in Fig.5.

$$x = \sqrt{\left(\frac{c}{a}\right)^2 - \left(\frac{c}{b}\right)^2 y^2} \quad (22)$$

Therefore, the present optimization can give a minor correction over Lechner's optimization only for a short instrument.

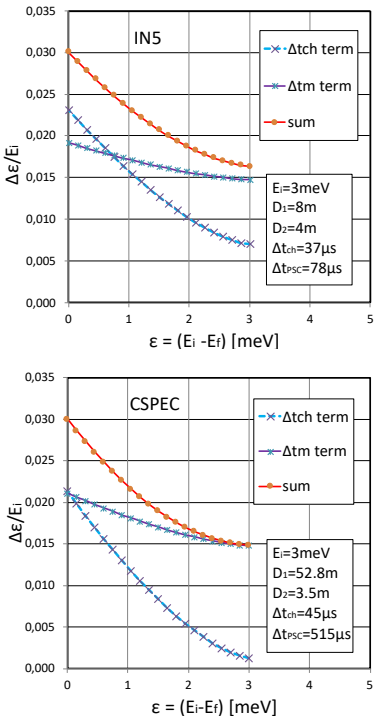

Fig. 6 Resolution diagram for the present optimization. Now the partial resolution regarding Δt_{ch} and Δt_m does not necessarily match at the elastic energy as seen in the panel of IN5, although that of CSPEC's has negligibly small change.

6 Estimated Flux of IN5, AMATERAS and CSPEC

Here, we estimate flux of IN5, AMATERAS and CSPEC on Typical Case.

In Table 1, we summarized the operation parameters in comparison with the Lechner's concept [1]. The difference is almost negligible for CSPEC but very small gain is found for IN5 which has a short d_i in comparison to CSPEC.

At the third bottom row in Table 1, the estimated absolute fluxes are listed. The IN5's flux of 6.44 X 10^5 is very closed to one listed in Ref. [10], and CSPEC's flux 2.64 X 10^6 is also very close to one in Ref. [8]. These results show the validity of the present calculation independently estimated from the brightness in Fig. 1 and give a base to make further estimates.

At the second bottom row, we can see that the performance of the single mode of AMATERAS [7] is almost comparable to CSPEC [8], and it is about four times higher than IN5 at 142 Hz operation [9], [10]. If we can reasonably utilize the RRM operation of CSPEC, we can have the performance shown at the bottom row, where the CSPEC's operation mode is assumed to be with 20% single mode and 80% of 6 - RRM mode giving a factor 5.0. But here we remark that AMATERAS regularly has 4 multi-Ei measurement, although the incident energy separation is well apart from each other as specified in Table 1 [7]. Therefore, the practical comparison between CSPEC and AMATERAS cannot simply estimated by the factor 5.0. RRM gives very different aspects for two instruments; CSPEC can increase statistics by adding RRM data in a certain range of incident energies, instead AMATERAS can observe a wide Q-E spectrum simultaneously.

Table 1. Parameters and performance in comparison with Lechner's concept [1], where the time averaged brightnesses for 1MW of J-PARC, 5MW of ESS and 57MW of ILL are taken as shown in Fig. 1.

Source	ILL (Lechner)	ILL (Present)	J-PARC	ESS (Lechner)	ESS (Present)	ESS
Time Averaged Brightness at 3meV, 5A, at the moderator surface [n/cm^2/s/str/eV]	2,09E+15	2,09E+15	2,0E+14	3,1E+15	3,1E+15	3,1E+15
Instrument operation mode	IN5 (142Hz)	IN5 (142Hz)	AMATERAS (single)	CSPEC (single)	CSPEC (single)	CSPEC (RRM) (single 20% + 6 RRM 80%)
d1 [m]	8	8	30	52,8	52,8	
d2 [m]	4	4	4	3,5	3,5	
d3 [m]	1,2	1,2	1,5	1,5	1,5	
Band width / frame [Å]			5,3	1,88	1,88	1,88
RRM or Multi-Ei	142 Hz	142 Hz	1,7 3,1 7,7 42,0 meV			2,2 2,4 2,6 3,0 3,4 3,9 meV
Monochro Chopper time Δtch [μs]	34	37	62	44,8	44,9	
Moderator or PSC time width Δtm [μs]	86	78	150	517,4	515,5	
2Δθ [deg]	2,0	2,0	2,0	2,0	2,0	
Δε[μeV] at elastic	90,0	90,0	90,0	90,0	90,0	
ΔEi[μeV]	52,5	49,1	24,6	44,7	44,5	
Flux (Estimated)	6,44E+05	6,55E+05	2,48E+06	2,64E+06	2,64E+06	1,32E+07
Ratio (1/AMATERAS)	0,26	0,26	1,0	1,07	1,07	5,34
Ratio /(CSPEC (Multi))	0,05	0,05	0,19	0,20	0,20	1,0

7 Optimization of d1

Because of constraint of a realistic dimension of the secondary spectrometer, d_2 could be 4 m and d_3 1.5 m, which achieves most of required resolution within a reasonable construction cost. However, d_1 is a kind of an optimizable length although we again need to consider the cost for a long guide. Here, we try to find an optimal length of d_1. Figure 7 shows the expected flux as a function of d_1 for Typical Case. Very interestingly the behavior of the flux curves have an opposite behavior in d_1 between AMATERAS and CSPEC or IN5. This is because Δt_m of AMATERAS is given, and shortening of d_1 makes Δt_{ch} a little shorter, and the argument in square-root of Eq. (5) has small reduction. But the division by d_1 in Eq. (5) eventually makes ΔE_i larger, and it makes a higher flux through Eq. (1). Contrarily to this, increasing d_1 for either CSPEC or IN5 makes increases both Δt_{ch} and Δt_{PSC}, but it cancels out with d_1 in the denominator in Eq. (5), and eventually ΔE_i stays almost constant independent from d_1 at a large d_1. Therefore, through Eq. (1) or Eq. (2), an increase of d_1 only makes gradual increase in the flux, and it shows a completely opposite d_1 dependences against one at a short pulse source.

For a long guide, however, we expect a beam loss. So, here, we show a very simple analysis of the beam loss through guide, where, we assumed a reflection performance parameter of $m = Q/Q_c(Ni) = 2$ with the critical refection factor of 0.94 with a 10 cm wide straight guide, which gives the required angular divergence of $\Delta\theta = \pm 1°$ at 5 Å [11]. The estimated flux of CSPEC multiplied by the beam loss is plotted in Fig. 7. It shows the flux above d_1 = 30 m does not have significant increase with d_1. However, since this estimate highly depends on the guide design and a detailed estimate should be necessary by using a computer simulation, and the present results should be taken just as a reference.

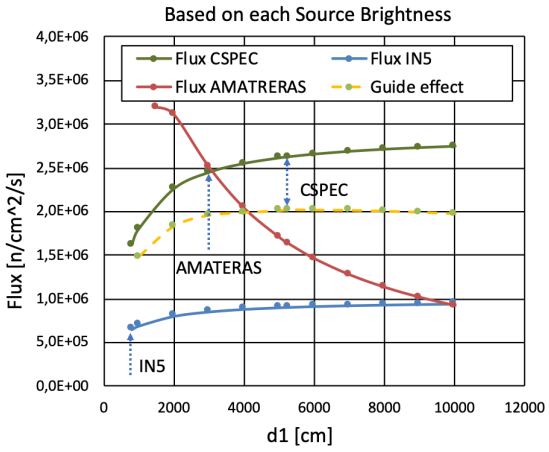

Fig. 7. Expected flux as a function of d_1 for a given resolution of 3% for Ei = 3meV for single mode.

From those results, it seems that CSPEC's d_1 = 52.8 m (PSC to sample) is a good choice, where flux increase tends to saturate. CSPEC has a 100 m guide-section before PSC from the moderator [8], which could make a beam loss of ca 20%, but can eliminate high energy neutrons and the spectrum is spread enough at PSC to have 6 RRM pulses. On the other hand, in case for IN5, d_1 seems to be too short and increasing d_1 to, say, 30 m may gain 20 - 30 % more flux, if the spatial constraint is not an issue. We have noticed a similar d_1 of 30 m was adapted to an upgrade of NEAT instrument giving a high performance [12].

AMATERAS had better to reduce d_1 as much as possible, however, this has a constraint given in Eq. (22). The widest Δt_m at practically lowest energy at 1 meV is 200 μs, therefore, the choice of d_1 = 30 m is also reasonable. However, for Typical Case of Ei = 3meV, a shorter distance of d_1 = 20 m gains 20 % more in flux.

8 Tunability in resolution and flux

So far, we have sticked on Typical Case. However, as we have noticed in Ref. [13], long pulse source inherently has a tunability in its resolution and flux. It can be also true even for spectrometers. Therefore, Fig. 8 shows the flux variation as a function of the energy

resolution at Ei = 3meV. Since Δt_m of AMATERAS is fixed to be 150 μs at 3meV, the available resolution range is very limited between 1,5% and 6%, below or above which Eq. (22) or Eq. (1) is not valid anymore because of negative Δt_{ch} or $\Delta t_{ch} > \Delta t_m$ respectively. On the other hand CSPEC and IN5 can choose almost freely the resolution in trade of flux because of a tunability in both Δt_{ch} and Δt_m. However, the maximum available resolution 15% of CSPEC is also limited by Δt_m= 2.96 ms of ESS's long pulse width. Because of this tunability, CSPEC and IN5 can have a very high flux by relaxing resolution, if it is demanded, which is inherently not available on AMATERAS.

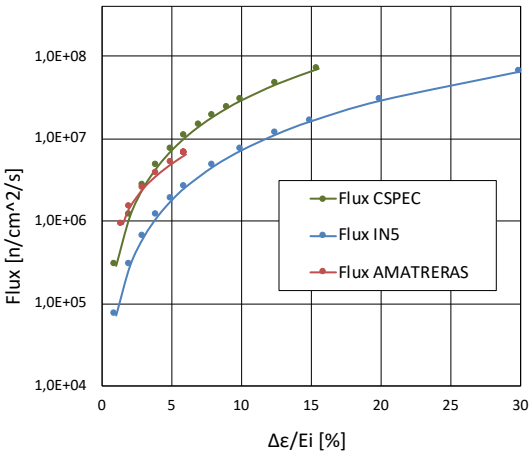

Fig. 8. Flux variation as a function of energy resolution.

9 Conclusion

In this report, I have developed a more precise optimization to determine Δt_{ch} and Δt_m of multi-chopper instrument. However, the result only gives a very minor improvement to a long d_i instrument over the well-known Lechner's optimization. It can only show an improvement to a short instrument, and an elongation of d_i of IN5 could gain another 20 to 30 % flux, if a spatial and cost constraint is not an issue. The analysis also showed that the choice of the current d_i of CSPEC and AMATERAS is very reasonable. The analysis showed how this class of instrument is suitable at a sharp pulse source for a high-resolution mode. However, CSPEC and IN5 has a great tunability in resolution and flux, giving various options from high resolution to high flux configuration covering a wide range of use cases, which is inherently difficult at a short pulsed source. Application of RRM of CSPEC could enhance its performance, although some detailed assessment could be necessary in terms of resolution effect by adding data of different wavelengths. On the other hand, AMATERAS has another class of multiplicity with multi-Ei, which gives a quick survey in a well separated Q-E space.

I acknowledge Dr. Ruep. E. Lechner very much, who made an outstanding guideline of design of this class of instrument, lead the community for a long time, and helped us to design CSPEC at ESS and AMATERAS at J-PARC.

10 References

1. R. E. Lechner, ICANS – XI International Collaboration on Advanced Neutron Sources, pp. 716–732 (1990)
2. M. Arai, L. Zanini, K. Andersen et al., Journal of Neutron Research, **22**, 71 (2020)
3. M. Russina and F. Mezei, Nuclear Instruments and Methods in Physics Research, **A604**, 624 (2009)
4. M. Nakamura, R. Kajimoto et al., Journal of the Physical Society of Japan, **78**(9), 093002 (2009)
5. M. Arai, Experimental Methods in the Physical Science, Volume 44, Chapter 3 pp. 245-320, Neutron Scattering-Fundamentals, Edited by Felix Fernandez-Alonso and David L. Price, (Elsevier Inc., 2014)
6. R. Lechner, Physica B, **276-278**,67 (2000)
7. K. Nakajima, S. Ohira-Kawamura et al, J. Phys. Soc. Jpn., **80**, SB028-1~ SB028-6, (2011)
8. K. Andersen et al., Nuclear Inst. and Methods in Physics Research, **A 957**, 163402 (2020)
9. J. Ollivier and H. Mutka, J. Phys. Soc. Jpn., **80**, SB003 (2011)
10. "Disk chopper time-of-flight spectrometer IN5": https://www.ill.eu/users/instruments/instruments-list/in5/description/instrument-layout .
11. "Super mirror" Swiss Neutronics, https://www.swissneutronics.ch/index.php?id=24.
12. M. Russina et al., Physica B: Condensed Matter **551**, 506 (2018)
13. M. Arai, K. Andersen, et al., Journal of Neutron Research, **23** (4), 215 (2021)